


Short-Term Variability of Proton Density Fat Fraction in Pancreas and Liver Assessed by Multiecho Chemical-Shift Encoding-Based MRI at 3 T

Jürgen Machann, PhD,^{1,2,3*}  Maytee Hasenbalg,¹ Julia Dienes, MD,⁴
Robert Wagner, MD,^{2,3,5} Arvid Sandforth, MD,^{2,3,5} Victor Fritz, MSc,¹
Andreas L. Birkenfeld, MD,^{2,3,5} Konstantin Nikolaou, MD,⁶ Stephanie Kullmann, PhD,^{2,3,5}
Fritz Schick, MD, PhD,¹ and Martin Heni, MD^{2,3,5,7}

Background: Quantification of pancreatic fat (PF) and intrahepatic lipids (IHL) is of increasing interest in subjects at risk for metabolic diseases. There is limited data available on short- and medium-term variability of PF/IHL and on their dependence on nutritional status.

Purpose: To assess short-term intraday variations of PF/IHL after a high-fat meal as well as medium-term changes after 5 days of high-caloric diet.

Study Type: Prospective cohort study.

Subjects: A total of 12 subjects (six males) for intraday variations study, 15 male subjects for medium-term high-caloric diet study and 11 age- and body mass index (BMI)-matched controls.

Field Strength/Sequence: A 3 T; chemical-shift encoded multiecho gradient echo sequence.

Assessment: For the intraday study, subjects were scanned after overnight fasting and after a high fat meal on the same day. For the medium-term study, 26 subjects were scanned after overnight fasting with 15/11 rescanned after 5 days of high-calorie diet/isocaloric diet. Proton density fat fraction (PDFF) maps were generated inline on the scanner. Regions of interest were manually drawn in head, body, and tail of pancreas and in the liver by a medical physicist and a doctoral student (26/4 years of experience). PF was calculated as the average of the head, body, and tail measurements.

Statistical Tests: Repeated measurements ANOVA for assessing changes in PF/IHL, linear correlation analyses for assessing relationships of PF/IHL with BMI. Significance level $P < 0.05$ for all.

Results: Nonsignificant changes in PF (2.6 ± 1.0 vs. $2.7 \pm 0.9\%$ after high-fat meal, 1.4 ± 0.8 vs. $1.5 \pm 0.6\%$ [high-caloric diet] and 1.5 ± 0.8 vs. $1.8 \pm 1.0\%$ [isocaloric control group]), nonsignificant changes in IHL after high-fat meal (2.6 ± 1.3 vs. $2.5 \pm 0.9\%$) and in the control group (1.1 ± 0.6 vs. $1.2 \pm 1.1\%$), significantly increased IHL after high-caloric diet ($1.7 \pm 2.2\%$ vs. $2.7 \pm 3.6\%$). Nonsignificant changes in PF (2.6 ± 1.0 vs. $2.7 \pm 0.9\%$ after high-fat meal, 1.4 ± 0.8 vs. $1.5 \pm 0.6\%$ [high-caloric diet] and 1.5 ± 0.8 vs. $1.8 \pm 1.0\%$ [isocaloric control group]), nonsignificant changes in IHL after high-fat meal (2.6 ± 1.3 vs. $2.5 \pm 0.9\%$) and in the control group (1.1 ± 0.6 vs. $1.2 \pm 1.1\%$), significantly increased IHL after 5-days of high-caloric diet ($1.7 \pm 2.2\%$ vs. $2.7 \pm 3.6\%$).

View this article online at [wileyonlinelibrary.com](https://onlinelibrary.wiley.com/doi/10.1002/jmri.28084). DOI: 10.1002/jmri.28084

Received Nov 11, 2021, Accepted for publication Jan 18, 2022.

*Address reprint requests to: J.M., Section on Experimental Radiology, Hoppe-Seyler-Str. 3, 72076 Tübingen, Germany.
E-mail: juergen.machann@med.uni-tuebingen.de

From the ¹Section on Experimental Radiology, Department of Diagnostic and Interventional Radiology, University Hospital, Tübingen, Germany; ²Institute for Diabetes Research and Metabolic Diseases (IDM) of the Helmholtz Center Munich at the University of Tübingen, Tübingen, Germany; ³German Center for Diabetes Research (DZD), Neuherberg, Germany; ⁴Department of Obstetrics and Gynecology, University of Tübingen, Tübingen, Germany; ⁵Department of Diabetology, Endocrinology and Nephrology, University Hospital, Tübingen, Germany; ⁶Department of Diagnostic and Interventional Radiology, University Hospital Tübingen, Germany; and ⁷Institute for Clinical Chemistry and Pathobiochemistry, Department for Diagnostic Laboratory Medicine, University Hospital Tübingen, Tübingen, Germany

This is an open access article under the terms of the Creative Commons Attribution-NonCommercial-NoDerivs License, which permits use and distribution in any medium, provided the original work is properly cited, the use is non-commercial and no modifications or adaptations are made.

Data Conclusion: Time of day and nutritional status have no significant influence on PF/IHL and are therefore not likely to be major confounders in epidemiologic or clinical studies.

Evidence Level: 2

Technical Efficacy: Stage 1

J. MAGN. RESON. IMAGING 2022.

Introduction

Due to the increasing prevalence of metabolic diseases—such as type 2 diabetes mellitus—and cardiovascular diseases, there is a rising interest in detailed phenotyping of persons at risk.¹ This is performed during interventions, including lifestyle modification,^{2–4} as well as in epidemiological studies in the general population such as in the Cooperative Health Research in the Augsburg Region,¹ the German National Cohort⁵ or the UK Biobank.⁶ For this purpose, MRI and proton MR spectroscopy (¹H-MRS) offer established and thorough techniques for quantification of whole-body adipose tissue distribution^{2,5} and assessment of ectopic fat deposition in abdominal organs, such as the liver and pancreas,⁷ and in skeletal muscle.⁸ Adipose tissue volume and distribution throughout the body, as well as ectopic fat accumulation in parenchymal tissues are important markers for, and presumably causative contributors to, individual metabolic risk.⁴ In this context, pancreatic fat (PF) and intrahepatic lipids (IHL) are of major interest, as they are linked to impaired glucose metabolism.^{9–13} For PF, an inverse correlation with insulin secretion has been shown in subjects with prediabetes^{9–11} and it has been hypothesized that PF modulates islet function in concert with further metabolic factors of the prediabetic milieu.¹² Furthermore, a reduction of PF, for example, by a dedicated lifestyle intervention, is thought to be important for improving pancreatic insulin secretion and the reversal of type 2 diabetes.¹³ IHL are negatively correlated with insulin sensitivity.¹⁴ Indeed, nonalcoholic fatty liver disease (NAFLD) is the most common cause of chronic liver disease, progressing to inflammation and fibrosis (nonalcoholic steatohepatitis),¹⁴ cirrhosis,¹⁵ liver failure and hepatocellular carcinoma.¹⁶ Even in normal weight subjects, fatty liver is a strong predictor for an unhealthy metabolism with increased risk for diabetes, cardiovascular events and mortality.¹⁷ IHL have therefore become one of the most important biomarkers in metabolic research.

Besides ¹H-MRS, multiecho gradient-echo chemical shift encoding-based techniques (CSE-MRI) have proven to be reliable for determination of proton density fat fraction (PDF) with some concomitant advantages. In contrast to ¹H-MRS, the entire volume of an organ can be assessed within a short measurement time (<20 s, i.e. in a single breath-hold) with adequate spatial resolution (<2 mm in-plane, <4 mm in slice-direction), allowing a detailed analysis and determination of intraorgan variabilities in fat-

distribution. In contrast, when applying single-voxel ¹H-MRS, information is obtained from a volume of several centimeters cubed. This is unproblematic in liver, as ectopic fat is evenly distributed, at least in subjects without liver pathologies,⁸ and repeated measurements, for example, in the course of a lifestyle intervention, allow reliable assessment of changes in IHL when recorded at the same position. For the pancreas however, due to its lobulated form, its location, stretching from behind the stomach to the left upper abdomen, and its inhomogeneous composition (ducts, exocrine and endocrine tissues, inhomogeneous fat distribution), spectroscopic examinations are challenging and in general are not advised. Even small movements of the subject or minor organ movement/displacement between morphologic imaging and spectroscopic data acquisition may lead to inclusion of signal from nearby visceral adipose tissue. Therefore, imaging approaches are favored for quantification of PF.

Intraday variations of ectopic lipids have been described for intramyocellular lipids (IMCL), revealing large fluctuations in response to nutritional status and physical exercise,²⁰ whereas IHL have been shown to be almost inert in respect of fasting/fed state.²¹ Data on short-term regulation of PF, however, are limited.

Thus, the aim of this study was to assess intrasession reproducibility and short-term intraday variations in PF/IHL after a high caloric meal, as well as medium-term changes after 5-days of high caloric diet.

Materials and Methods

Subjects

The studies were approved by the local ethics committee and written informed consent was obtained from all subjects.

Study Design

INTRASESSION REPRODUCIBILITY AND INTRADAY VARIABILITY. Twelve healthy subjects (six males, age: 24–49 years, body mass index (BMI): 19.2–27.8 kg/m²) were enrolled. To test for intrasession reproducibility and intraday variability of PF and IHL, three examinations were performed (Fig. 1a). The first MR examination was done in the early morning after overnight fasting, and a second MR examination was then performed within the same session after new positioning and adjustment of the scanner. The third examination followed at lunchtime, 1 hour after ingestion of an energy dense meal (pizza, containing 5100–7300 kJ, 52–93 g fat, 123–163 g carbohydrate) and a sweetened soft-drink (containing 53 g carbohydrate).

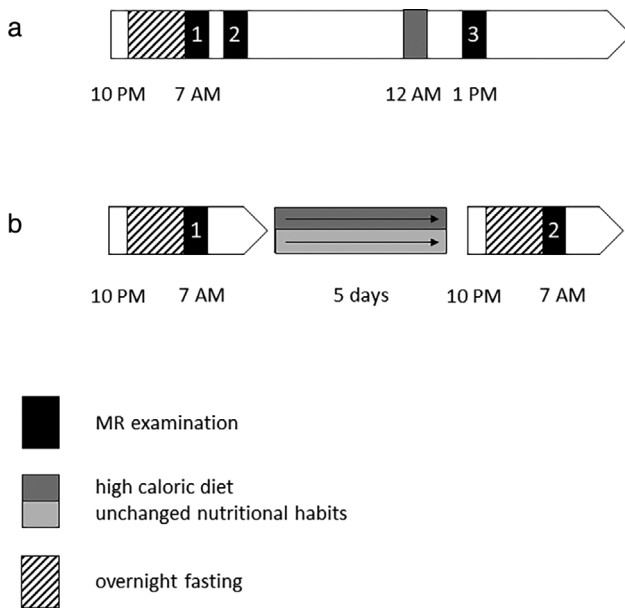


FIGURE 1: Flowchart for repeated CSE-MRI in the framework of determination of intraday variabilities (a) and a 5-day high-caloric diet (b).

VARIABILITY AFTER 5 DAYS OF HIGH-CALORIC DIET. To assess medium-term changes in PF and IHL, 15 healthy male subjects (age: 19–27 years, BMI: 18.6–24.4 kg/m²) underwent a high-caloric diet for 5 days with a daily surplus of 6200 kJ on their individual basal metabolic rate. Additionally, 11 age- and BMI-matched males (age: 20–26 years, BMI: 19.9–24.0 kg/m²) were examined twice with the same time difference between the MR measurements and without changing their nutritional habits. Females were not included in this study in order to avoid possible interference of effects of menstrual cycle and/or sex hormones on body fat distribution. MR examinations were performed in the early morning after an overnight fasting period at baseline and after the 5-day interval (Fig. 1b). All participants were instructed to maintain their normal behavior regarding physical activity and hydration during this period.

MR EXAMINATIONS—STUDY PROTOCOL. MR examinations were performed on a 3 T whole-body scanner (Magnetom Vida, Siemens Healthineers, Erlangen, Germany). Subjects were placed head first in supine position with the spine-array coil mounted on the patient table of the scanner. Additionally, an 18-channel body-array coil was used for homogeneous coverage of the upper abdomen. After morphologic imaging, a 3D multiecho CSE sequence was acquired covering the entire liver and pancreas with the following parameters: matrix size 160 × 132, field-of-view 380 × 314 mm, partition thickness 3 mm (80 partitions in total), repetition time TR = 8.9 msec, six echoes with echo times TE = 1.09, 2.46, 3.69, 4.92, 6.15, and 7.38 msec, flip angle 4°, acceleration Caipirinha, factor 2 in both, phase-encoding and slice encoding directions, bandwidth 1080 Hz/pixel, acquisition time TA = 17 seconds (breath-hold). PDFF-maps were generated inline on the console of the scanner as described,^{19,22} correcting for microscopic magnetic field inhomogeneities by correction for T2*. In this PDFF-map, intensity values directly reflect PF and IHL in percent. To assess the feasibility of the CSE sequence to detect changes in the low range of PDFF, an in vitro experiment was

performed using fat/water emulsions of different concentrations ranging from 1.0% to 3.2% in steps of 0.2%, as well as 4%, 5%, 10%, and 30% as shown in the axial T1-weighted fast spin-echo image in Fig. 2a. Emulsions were prepared in CELLSTAR polypropylene tubes (Greiner Bio-One, Frickenhausen, Germany) with a volume of 50 mL, filled with distilled water and peanut oil. Soy lecithin was used as an emulsifier to obtain stable and homogenous emulsions.²³ The tubes were placed in horizontal direction in a water bath. Sequence parameters were identical to the in vivo measurements except TR, which was set to 20 msec to avoid T1-bias. Furthermore, in subjects participating in the medium-term high caloric diet study a single voxel STEAM spectroscopy was applied in the posterior part of segment 7 of the liver. Spectra were recorded with TE = 20 msec, TR = 4 seconds, 16 acquisitions with two prescans in a VOI of 3 × 3 × 2 cm³ after automatic shimming. Subjects were asked to hold expiration during data acquisition to minimize breathing effects.

POSTPROCESSING. Quantification of PF and IHL was performed by two independent operators (JM, 26 years of experience in MRI; MHa, 4 years of experience in MRI) by manually drawing circular regions of interest (ROI) in the PDFF maps. Three small circular ROIs were defined in the pancreas, one in the head (PF_H, Fig. 3a), one in the body (PF_B) and one in the tail (PF_T), both Fig. 3b, carefully avoiding inclusion of surrounding visceral adipose tissue. The mean value of the three ROI's was calculated (PF_{mean}). Where necessary, evaluation of the three pancreatic subregions was performed in different axial slices due to the lobulated form of the organ. Owing to the almost homogeneous distribution of fat in the liver, a larger volume of interest (VOI) with a diameter of approximately 3 cm was defined in the posterior part of Couinaud-segment 7 (see Fig. 2c), carefully selecting the ROI in the identical position at the follow-up examinations and corresponding to the placement of VOI in MRS. Chosen ROI's of the first measurement were available to the respective operator at the time of the second measurement but blinded for determination of interobserver variability.

Spectroscopic raw data were exported to a standalone PC. Integrals of water signal at 4.7 ppm and main lipid signals (methyl at 0.9 ppm and methylene at 1.3 ppm) were quantified as described.² The ratio of the signal integrals of lipids (methylene + methyl) and signal integrals of water + lipids was calculated and IHL_{MRS} are expressed in percent.

STATISTICS. Statistical analyses were performed with JMP (JMP® 15.2.0 SAS Institute, Cary, NC). Data are reported as mean ± SD unless otherwise stated. Evaluation of the effect of variabilities in ectopic fat compartments (PF_{mean} and IHL) was performed by a two-way repeated measurement ANOVA analysis with a significance level set to $P < 0.05$. Univariate linear correlation analyses were used to analyze the coefficient of determination (R^2) between PF, IHL and BMI. P values < 0.05 were considered statistically significant. To assess the interobserver variability, the intraclass correlation coefficient (ICC) was calculated.

Results

In all examinations, PDFF-maps could be generated free of potential motion-artifacts or phase wrapping, thus being reliable for quantification of PF and IHL.

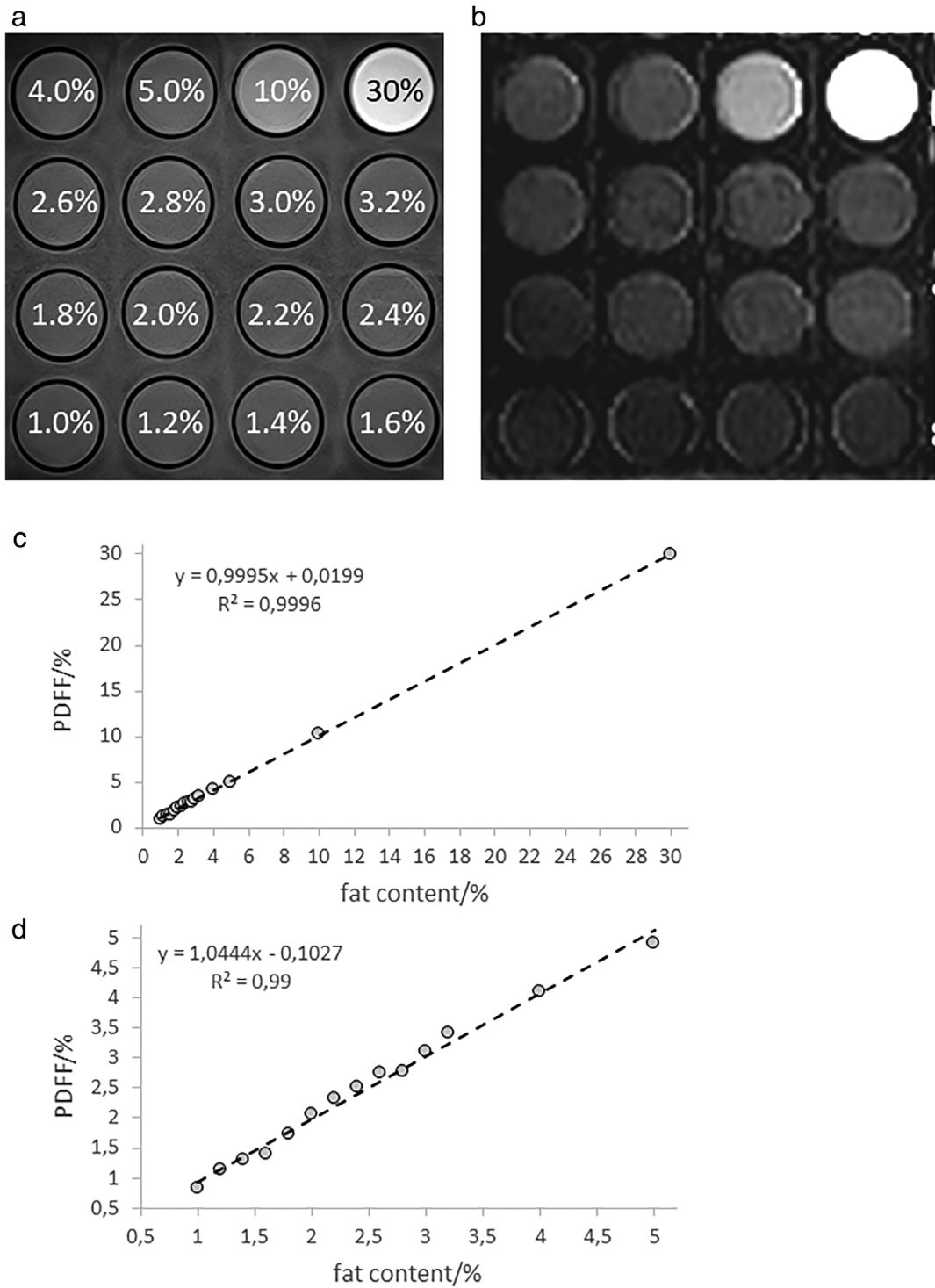


FIGURE 2: (a) T1-weighted axial image of the tubes filled with emulsions of different oil concentration as indicated. (b) PDFF-map calculated from the applied CSE-sequence. (c) Correlation between nominal fat concentration and the resulting PDFF (full range) and (d) correlation between nominal fat concentration and the resulting PDFF (1%–5%).

Interrater variability resulted in an ICC of 0.93 for ROIs selected in pancreas and 0.99 for ROIs selected in liver. All further analyses were performed using the means of the two observers.

Comparison of CSE-derived PDFF values and IHL_{MRS} in the liver resulted in a high correlation

($R^2 = 0.98$ for the entire range of PDFF, i.e. 0.3%–14.6%), $R^2 = 0.91$ for low PDFF < 5%). Subsequently, results from the imaging technique are given, as MRS was limited to liver.

The in vitro measurement of the emulsions with variable fat content revealed consistency for all chosen

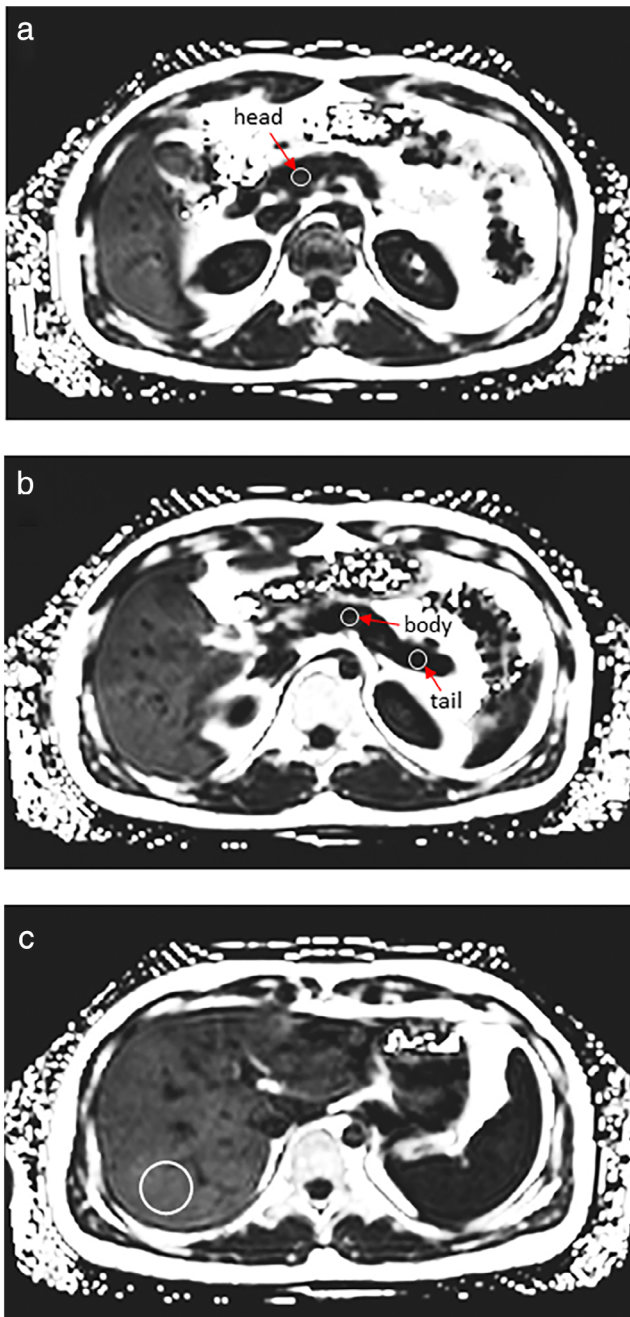


FIGURE 3: Axial PDFF-maps from a 23-year-old male subject indicating ROIs for evaluation of pancreatic proton density fat fraction (PF) in head (a), body and tail (b) as well as from intrahepatic lipids (IHL, c).

concentrations (i.e. 1%–30% as indicated in Fig. 2a). Figure 2b shows the corresponding PDFF map. The determined PDFF-values are shown in Fig. 2c for the entire range of concentrations and in Fig. 2d for low PDFF values up to 5%—both approximating identity with minor deviations. Bright spots in the background (water) and at the border of the vials are mainly attributed to susceptibility artifacts resulting at the transition between the grid for placement of the tubes and the casing of the tubes.

Intraday Variability

Analysis of pancreatic fat in the 12 participating subjects revealed slight regional differences ($2.0\% \pm 0.8\%$, $2.9\% \pm 1.6\%$, and $2.9\% \pm 1.3\%$ for PF_H , PF_B and PF_T , respectively; significant for PF_H and PF_B , $P = 0.07$ between PF_H and PF_T and $P = 0.96$ between PF_B and PF_T) in the first examination. Repeated measurement after new positioning and adjustment of the scanner resulted in similar PDFF values (2.0 ± 0.8 , 2.9 ± 1.5 , 2.9 ± 1.4 for PF_H , PF_B , and PF_T , respectively) with a coefficient of variation (CV) of 0.3% for PF_H , 0.1% for PF_B , and 0.8% for PF_T . After the high-fat meal—Fig. 4 shows images at the same position in the fasting state (Fig. 4a) and with fully loaded stomach after the meal (Fig. 4b)—, there were no significant changes in PF_H ($2.1\% \pm 0.8\%$, $P = 0.52$), PF_B ($2.8\% \pm 1.6\%$, $P = 0.46$) or PF_T ($3.0\% \pm 1.3\%$, $P = 0.08$) as determined by repeated measurement ANOVA analysis. The PF_{mean} values were $2.6\% \pm 1.0\%$, $2.6\% \pm 0.9\%$, and $2.7\% \pm 0.9\%$ for examinations 1, 2, and 3, respectively and were not statistically significantly different ($P = 0.26$ for 1 vs. 2, 0.34 for 1 vs. 3, and 0.54 for 2 vs. 3). Individual changes in PF_{mean} are shown in Fig. 5a (left side).

An almost similar pattern of results was obtained in the liver with IHL of $2.6\% \pm 1.3\%$ in the first measurement, $2.6\% \pm 1.3\%$ for the repeated measurement after new adjustment of the scanner (CV = 0.4%, $P = 0.69$) and $2.5\% \pm 1.3\%$ 1 hour after the high-fat meal ($P = 0.16$). Individual results are shown in Fig. 4a (right side).

Variability after 5 Days of High-caloric Diet

Before the dietary intervention, the regional distribution of PF in the 15 subjects participating in the 5-days high-caloric diet revealed a homogeneous pattern with $PF_H/PF_B/PF_T$ of $1.4\% \pm 1.0\%/1.4\% \pm 0.9\%/1.4\% \pm 1.1\%$ with PF_{mean} averaging to $1.4\% \pm 0.8\%$. This pattern was slightly shifted after the dietary intervention resulting in $1.6\% \pm 0.9\%$ for PF_H ($P = 0.09$), $1.5\% \pm 0.7\%$ for PF_B ($P = 0.46$), and $1.4\% \pm 0.9\%$ for PF_T ($P = 0.88$), indicating a minimal mean increase in pancreatic head and body but being unchanged in body and tail. Thus, PF_{mean} slightly increased from $1.4\% \pm 0.8\%$ at baseline to $1.5\% \pm 0.6\%$ after the high-caloric diet ($P = 0.21$). Individual courses for PF_{mean} are displayed (Fig. 5b, left side).

IHL increased significantly from $1.7\% \pm 2.2\%$ (range: 0.4%–8.8%) to $2.7\% \pm 3.6\%$ (range: 0.5%–15.0%). Twelve of the subjects increased their IHL and 3 showed a marginal decrease as shown in Fig. 5b on the right side.

Within the control group of subjects not changing their dietary habits during this interval, there was a slight but non-significant increase in PF_{mean} from $1.6\% \pm 1.2\%$ to $1.8\% \pm 1.4\%$ ($P = 0.51$). IHL were unchanged ($1.1\% \pm 0.6\%$ at baseline vs. $1.2\% \pm 1.1\%$, $P = 0.45$).

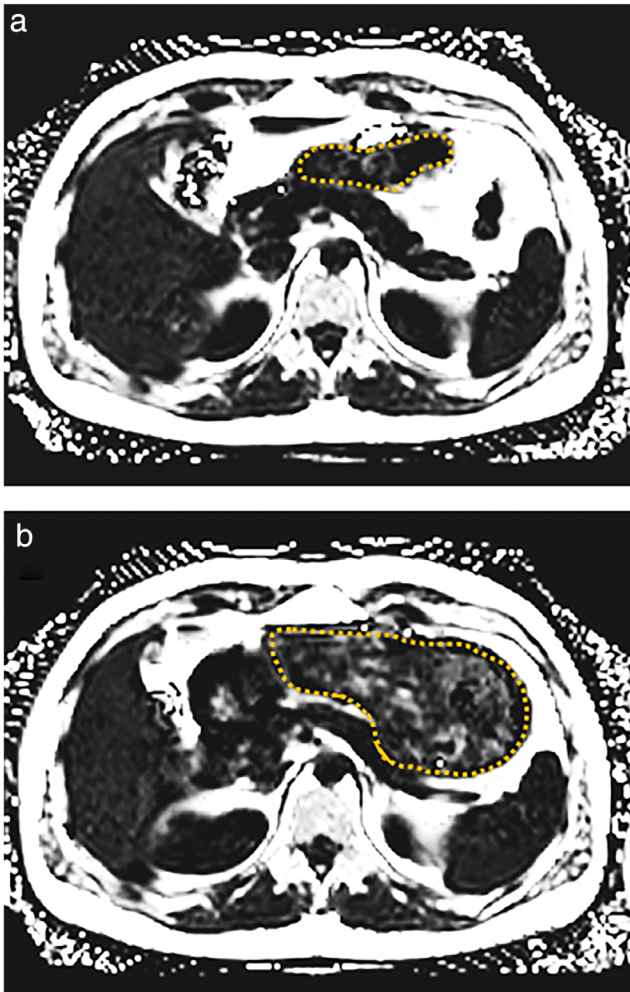


FIGURE 4: Axial PDFF-maps from a 29-year-old male subject prior to (a) and after high-fat meal (b) highlighting challenges of positioning the ROI due to the filled stomach (dashed line) at the second examination.

There was a weak but significant positive correlation between PF_{mean} and IHL in the combined subjects from both studies ($N = 38$) with an R^2 of 0.20 as shown in Fig. 6a. Whereas PF did not show an association with BMI ($R^2 = 0.11$, $P = 0.06$), IHL showed a significant correlation with BMI ($R^2 = 0.26$) as shown in Fig. 6b,c.

Discussion

CSE-MRI allows sensitive quantification of ectopic lipid deposition in various organs. Even low concentrations can be assessed and marginal differences and/or changes are observable as supported by the in vitro experiments in this study. It has to be mentioned that these results are probably not directly transferable to in vivo measurements, where noise contributions in regions with very low PDFF have to be taken into consideration as shown by Hong et al.²⁴

Our intraday study showed minor nonsignificant changes in PF after a high-fat meal, as well as minor nonsignificant changes after 5 days of high-caloric diet. Hence, PF is likely a relatively inert ectopic fat depot. In contrast, IHL were significantly increased after the 5-day-dietary challenge, suggesting a more rapid accumulation of fat in the liver. Short-term (intrasession) reproducibility of PF and IHL was very good, as was medium-term reproducibility in the control group after 5 days of unchanged dietary habits.

When planning cross-sectional or longitudinal studies that aim to quantify PF or IHL, it is often discussed whether the MR examinations have to be performed in a standardized manner, for example, in the early morning after overnight fasting or with a special dietary program in the days prior to measurements. Our current data indicate that time of day and nutritional status have no major impact.

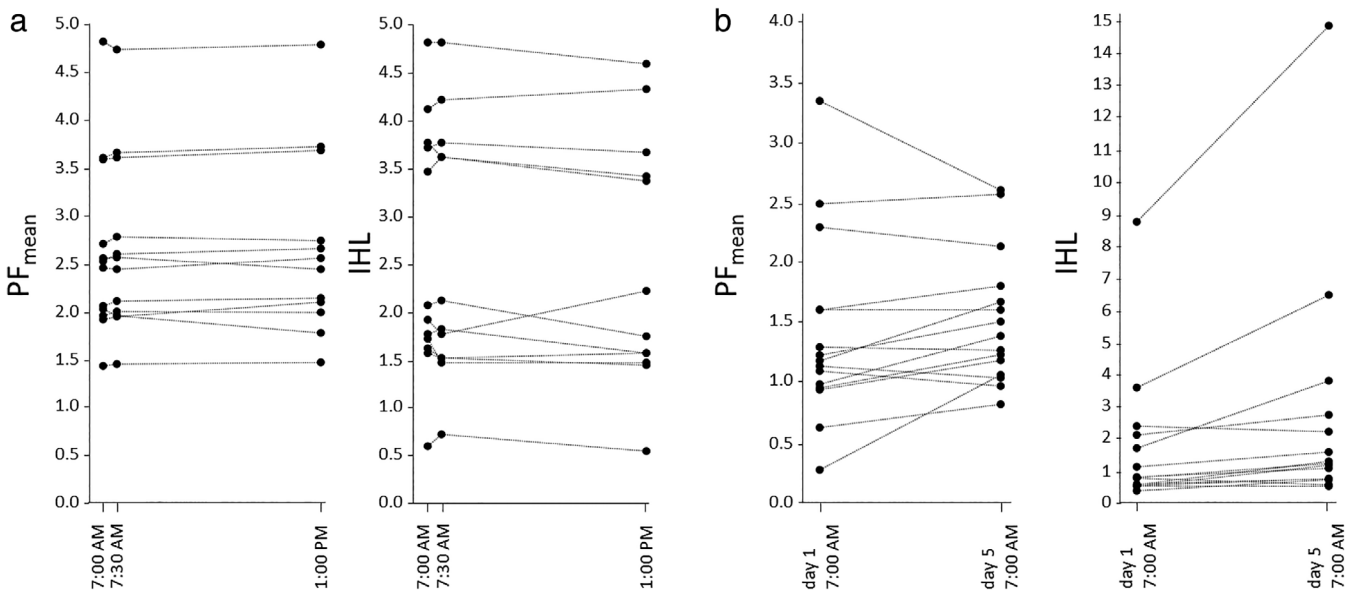


FIGURE 5: Individual variations of PF_{mean} (left) and IHL (right) in the course of repeated CSE-MRI. (a) Intraday variabilities, (b) 5 days of high-caloric diet.

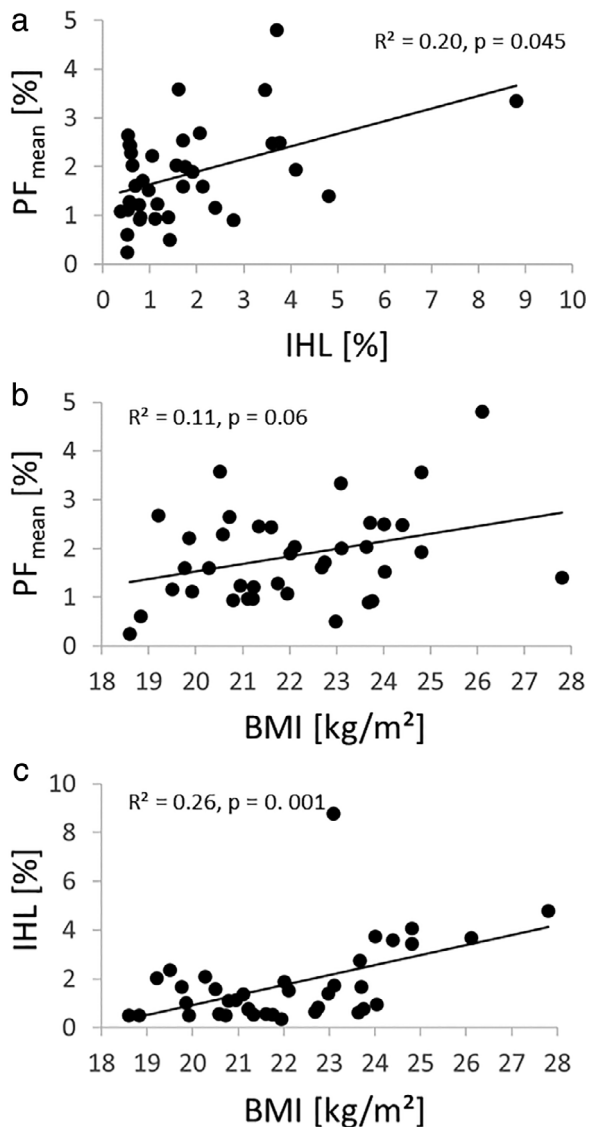


FIGURE 6: Linear regression between PF_{mean} and IHL (a), BMI and PF_{mean} (b) and BMI and IHL (c) reveal a significant correlation between PF_{mean} and IHL and a significant positive correlation between BMI and PDFF in liver.

Quantification of ectopic lipids, for example, in skeletal muscle (IMCL), liver (IHL) or pancreas (PF) has gained a lot of interest in cross-sectional and longitudinal studies as ectopic lipid accumulation is a well-known important contributor to the pathogenesis of metabolic diseases.^{2,4,8–11} Thus, noninvasive MR-based phenotyping including fat quantification is increasingly being applied in large-scale epidemiological studies as well as in interventional prospective studies.^{1,4,5,13} In contrast to the major adipose tissue compartments (subcutaneous fat and visceral fat), quantification of ectopic lipids in organs which—under healthy circumstances—contain little or no fat is more challenging and requires special techniques for exact assessment. Volume localized MRS has proven to be a reliable method, allowing a detailed analysis of characteristic metabolites in a specific

tissue, for example, IMCL, which have shown fast regulation in the course of short-term dietary intervention,²⁵ fasting,²⁶ or even in the course of the day.²⁰ For quantification of IHL, ¹H-MRS was the noninvasive reference standard,²⁷ but this is now being replaced by CSE-based MRI.

Due to the irregular lobulated shape and inhomogeneous fat distribution in the pancreas, ¹H-MRS is not recommended for quantification of PF.²⁸ Furthermore, availability of ¹H-MRS is limited, whereas CSE-based MRI-techniques are increasingly obtainable. Two-point Dixon techniques are not suitable for this purpose as they do not allow the calculation of PDFF and can therefore only serve as a screening method to detect hepatic steatosis.²⁹

CSE-based MRI is distinguished by excellent linearity, accuracy, and reproducibility, which has been shown in phantoms at different field strength and for different manufacturers³⁰ as well as for in vivo applications.^{31,32} Thus, its application for accurate quantification of PF in cross-sectional or interventional studies is recommended. Whereas the acquisition strategy is well established, standardized evaluation of the PDFF-maps is still under debate. While the manual drawing of ROIs in pancreatic head, body and tail allows detection of regional variability of PF,^{10,33,34} this approach is prone to interobserver discrepancies and volumetric (3D) analysis has improved repeatability and reproducibility.³⁵ Al-Mrabeh et al proposed a so-called “MR-opsy” approach, excluding signal contributions from pancreatic ducts and intrusions of visceral fat by thresholding and thereby excluding nonparenchymal tissue.³⁶ In combination with automatic organ segmentation by deep-learning-based algorithms,³⁷ this might promise a fast and user-independent postprocessing procedure in the future.

There is little information available about short-term variations of PF. Regarding longer-term changes, a decrease of PF has been described after laparoscopic sleeve gastrectomy,³⁸ after gastric bypass surgery in patients with type 2 diabetes mellitus, but not in subjects with normal glucose tolerance³⁹ and following diet-induced weight loss,⁴⁰ but there is no information about changes in PF after high-fat/high-caloric diet. Long-term regulation of IHL after dietary lifestyle intervention is well known and has been described in the literature,^{2,4,13,38} but little is known about the period when this reduction becomes evident.

Limitations

The generalizability of our findings is limited as we included only healthy and rather lean young subjects with relatively low PF and IHL; only one subject, who showed the strongest increase after the high-caloric diet, fulfilled the criteria for fatty liver (i.e. IHL > 5.56%²⁷). Thus, it remains to be determined whether or not subjects with higher ectopic fat content (eg persons at risk for metabolic diseases, overweight/obese subjects or patients with type 2 diabetes mellitus) reveal larger variations under similar conditions. Only males were included

in the diet intervention study. Even if there is no indication of different responses to food intake between sexes, this study can certainly not exclude such effects. Furthermore, we only evaluated two time-points in the intraday study and can therefore not rule out variations at later time points after the meal or following a longer fasting period.

Another point which has to be addressed is, that this study was restricted to high-caloric and high-fat interventions. Whether or not there are short-term changes after prolonged starvation or after exercise as previously detected for IMCL²⁰ cannot be answered from our data.

Manual analysis bears potential for inaccuracies in post-processing at least in the pancreas, which is characterized by an inhomogeneous fat distribution. However, the high inter-rater concordance supports the reliability of our results.

Finally, it has to be mentioned that the reproducibility in selection of the ROIs in pancreas after ingestion of the meal was aggravated by relocation of the pancreas due to the fully loaded stomach as shown in Fig. 4.

Conclusion

There were no significant short-term (intraday) variations in PF or IHL in healthy lean subjects, regardless of nutritional status. After 5-days of high-calorie diet, PF was unchanged, whereas IHL was significantly increased.

Acknowledgments

The authors thank all study participants for their contribution and the members of Siemens Healthineers for continuous support. Supported in part by a grant (01GI0925) from the German Federal Ministry of Education and Research (BMBF) to the German Center for Diabetes Research (DZD e.V.)

Open access funding enabled and organized by Projekt DEAL.

REFERENCES

- Bamberg F, Hetterich H, Rospleszcz S, et al. Subclinical disease burden as assessed by whole-body MRI in subjects with prediabetes, subjects with diabetes, and Normal control subjects from the general population: The KORA-MRI study. *Diabetes* 2017;66:158-169.
- Machann J, Thamer C, Stefan N, et al. Follow-up whole-body assessment of adipose tissue compartments during a lifestyle intervention in a large cohort at increased risk for type 2 diabetes. *Radiology* 2010; 257:353-363.
- Cordes C, Dieckmeyer M, Ott B, et al. MR-detected changes in liver fat, abdominal fat, and vertebral bone marrow fat after a four-week calorie restriction in obese women. *J Magn Reson Imaging* 2015;42:1272-1280.
- Fritsche A, Wagner R, Heni M, et al. Risk-stratified lifestyle intervention to prevent type 2 diabetes results of the randomized controlled prediabetes lifestyle intervention study (PLIS). *Diabetes* 2021;70(12):2785-2795.
- Bamberg F, Kauczor HU, Weckbach S, et al. Whole-body MR imaging in the German National Cohort: Rationale, design, and technical background. *Radiology* 2015;277:206-220.
- Wilman HR, Kelly M, Garratt S, et al. Characterisation of Liver Fat in the UK Biobank cohort. *PLoS One* 2017;12:e0172921.
- Hong CW, Fazeli Dehkordy S, Hooker JC, Hamilton G, Sirlin CB. Fat quantification in the abdomen. *Top Magn Reson Imaging* 2017;26(6): 221-227.
- Machann J, Stefan N, Schick F. 1H MR spectroscopy of skeletal muscle, liver and bone marrow. *Eur J Radiol* 2008;67:275-284.
- Tushuizen ME, Bunck MC, Pouwels PJ, et al. Pancreatic fat content and β -cell function in men with and without type 2 diabetes. *Diabetes Care* 2007;30:2916-2921.
- Heni M, Machann J, Staiger H, et al. Pancreatic fat is negatively associated with insulin secretion in individuals with impaired fasting glucose and/or impaired glucose tolerance: A nuclear magnetic resonance study. *Diabetes Metab Res Rev* 2010;26:200-205.
- Wagner R, Jaghutriz BA, Gerst F, et al. Pancreatic steatosis associates with impaired insulin secretion in genetically predisposed individuals. *J Clin Endocrinol Metab* 2020;105:3518-3525.
- Wang CY, Ou HY, Chen MF, Chang TC, Chang CJ. Enigmatic ectopic fat: Prevalence of nonalcoholic fatty pancreas disease and its associated factors in a Chinese population. *J Am Heart Assoc* 2014;3: e000297.
- Taylor R, Al-Mrabeh A, Zhyzhneuskaya S, et al. Remission of human type 2 diabetes requires decrease in liver and pancreas fat content but is dependent upon capacity for β cell recovery. *Cell Metab* 2018;28: 547-556.
- Stefan N, Häring HU, Cusi K. Non-alcoholic fatty liver disease: Causes, diagnosis, cardiometabolic consequences, and treatment strategies. *Lancet Diabetes Endocrinol* 2019;7:313-324.
- Farrell GC, Larter CZ. Nonalcoholic fatty liver disease: From steatosis to cirrhosis. *Hepatology* 2006;43(2 Suppl 1):S99-S112.
- Nahon P, Allaire M, Nault JC, Paradis V. Characterizing the mechanism behind the progression of NAFLD to hepatocellular carcinoma. *Hepat Oncol* 2020;7:HEP36.
- Stefan N, Schick F, Häring HU. Causes, characteristics, and consequences of metabolically unhealthy Normal weight in humans. *Cell Metab* 2017;26:292-300.
- Idilman IS, Aniktar H, Idilman R, et al. Hepatic steatosis: Quantification by proton density fat fraction with MR imaging versus liver biopsy. *Radiology* 2013;267:767-775.
- Zhong X, Nickel MD, Kannengiesser SA, Dale BM, Kiefer B, Bashir MR. Liver fat quantification using a multi-step adaptive fitting approach with multi-echo GRE imaging. *Magn Reson Med* 2014;72:1353-1365.
- Machann J, Etzel M, Thamer C, et al. Morning to evening changes of intramyocellular lipid content in dependence on nutrition and physical activity during one single day: A volume selective (1)H-MRS study. *Magn Reson Mater Phy* 2011;24:29-33.
- Colgan TJ, Van Pay AJ, Sharma SD, Mao L, Reeder SB. Diurnal variation of proton density fat fraction in the liver using quantitative chemical shift encoded MRI. *J Magn Reson Imaging* 2020;51:407-414.
- Bashir MR, Zhong X, Nickel MD, et al. Quantification of hepatic steatosis with a multistep adaptive fitting MRI approach: Prospective validation against MR spectroscopy. *Am J Roentgenol* 2015;204:297-306.
- Fritz V, Martirosian P, Machann J, Daniels R, Schick F. A comparison of emulsifiers for the formation of oil-in-water emulsions: Stability of the emulsions within 9 h after production and MR signal properties. *Magn Reson Mater Phy* 2021. <https://doi.org/10.1007/s10334-021-00970-9>. Online ahead of print.
- Hong CW, Hamilton G, Hooker C, et al. Measurement of spleen fat on MRI-proton density fat fraction arises from reconstruction of noise. *Abdom Radiol* 2019;44(10):3295-3303.
- Bachmann OP, Dahl DB, Brechtel K, et al. Effects of intravenous and dietary lipid challenge on intramyocellular lipid content and the relation with insulin sensitivity in humans. *Diabetes* 2001;50:2579-2584.

26. Wietek BM, Machann J, Mader I, et al. Muscle type dependent increase in intramyocellular lipids during prolonged fasting of human subjects: A proton MRS study. *Horm Metab Res* 2004;36:639-644.
27. Szczepaniak LS, Nurenberg P, Leonard D, et al. Magnetic resonance spectroscopy to measure hepatic triglyceride content: Prevalence of hepatic steatosis in the general population. *Am J Physiol Endocrinol Metab* 2005;288:E462-E468.
28. Hu HH, Kim HW, Nayak KS, Goran MI. Comparison of fat-water MRI and single-voxel MRS in the assessment of hepatic and pancreatic fat fractions in humans. *Obesity (Silver Spring)* 2010 Apr;18(4):841-847.
29. Zhan C, Olsen S, Zhang HC, Kannengiesser S, Chandarana H, Shanbhogue KP. Detection of hepatic steatosis and iron content at 3 tesla: Comparison of two-point Dixon, quantitative multi-echo Dixon, and MR spectroscopy. *Abdom Radiol*. 2019;44(9):3040-3048.
30. Hu HH, Yokoo T, Bashir MR, et al. Linearity and bias of proton density fat fraction as a quantitative imaging biomarker: A multicenter, multiplatform multivendor phantom study. *Radiology* 2021;298:640-651.
31. Artz NS, Haufe WM, Hooker CA, et al. Reproducibility of MR-based liver fat quantification across field strength: Same-day comparison between 1.5T and 3T in obese subjects. *J Magn Reson Imaging* 2015; 42:811-817.
32. Wu B, Han W, Li Z, et al. Reproducibility of intra- and inter-scanner measurements of liver fat using complex confounder-corrected chemical shift encoded MRI at 3.0 tesla. *Sci Rep* 2016;6:19339.
33. Li J, Xie Y, Yuan F, Song B, Tang C. Noninvasive quantification of pancreatic fat in healthy male population using chemical shift magnetic resonance imaging: Effect of aging on pancreatic fat content. *Pancreas* 2011;40:295-299.
34. Heber SD, Hetterich H, Lorbeer R, et al. Pancreatic fat content by magnetic resonance imaging in subjects with prediabetes, diabetes, and controls from a general population without cardiovascular disease. *PLoS One* 2017;12:e0177154.
35. Kato S, Iwasaki A, Kurita Y, et al. Three-dimensional analysis of pancreatic fat by fat-water magnetic resonance imaging provides detailed characterization of pancreatic steatosis with improved reproducibility. *PLoS One* 2019;14:e0224921.
36. Al-Mrabeh A, Hollingsworth KG, Steven S, Tiniakos D, Taylor R. Quantification of intrapancreatic fat in type 2 diabetes by MRI. *PLoS One* 2017;12:e0174660.
37. Isensee F, Jaeger PF, Kohl SAA, Petersen J, Maier-Hein KH. nnU-net: A self-configuring method for deep learning-based biomedical image segmentation. *Nat Methods* 2021;18:203-211.
38. Covarrubias Y, Fowler KJ, Mamidipalli A, et al. Pilot study on longitudinal change in pancreatic proton density fat fraction during a weight-loss surgery program in adults with obesity. *J Magn Reson Imaging* 2019;50:1092-1102.
39. Steven S, Hollingsworth KG, Small PK, et al. Weight loss decreases excess pancreatic triacylglycerol specifically in type 2 diabetes. *Diabetes Care* 2016;39:158-165.
40. Jiang Y, Spurny M, Schübel R, et al. Changes in pancreatic fat content following diet-induced weight loss. *Nutrients* 2019; 11:912.